Moss and liverwort xyloglucans contain galacturonic acid and are structurally distinct from the xyloglucans synthesized by hornworts and vascular plants*

Maria J Peña[1,2], Alan G. Darvill[2,3], Stefan Eberhard[2], William S York[2,3], and Malcolm A O'Neill[2]

[2]Complex Carbohydrate Research Center; and [3]Department of Biochemistry and Molecular Biology, University of Georgia, Athens, GA 30602, USA

Xyloglucan is a well-characterized hemicellulosic polysaccharide that is present in the cell walls of all seed-bearing plants. The cell walls of avascular and seedless vascular plants are also believed to contain xyloglucan. However, these xyloglucans have not been structurally characterized. This lack of information is an impediment to understanding changes in xyloglucan structure that occurred during land plant evolution. In this study, xyloglucans were isolated from the walls of avascular (liverworts, mosses, and hornworts) and seedless vascular plants (club and spike mosses and ferns and fern allies). Each xyloglucan was fragmented with a xyloglucan-specific endo-glucanase and the resulting oligosaccharides then structurally characterized using NMR spectroscopy, MALDI-TOF and electrospray mass spectrometry, and glycosyl-linkage and glycosyl residue composition analyses. Our data show that xyloglucan is present in the cell walls of all major divisions of land plants and that these xyloglucans have several common structural motifs. However, these polysaccharides are not identical because specific plant groups synthesize xyloglucans with unique structural motifs. For example, the moss *Physcomitrella patens* and the liverwort *Marchantia polymorpha* synthesize XXGGG- and XXGG-type xyloglucans, respectively, with sidechains that contain a β-D-galactosyluronic acid and a branched xylosyl residue. By contrast, hornworts synthesize XXXG-type xyloglucans that are structurally homologous to the xyloglucans synthesized by many seed-bearing and seedless vascular plants. Our results increase our understanding of the evolution, diversity, and function of structural motifs in land-plant xyloglucans and provide support to the proposal that hornworts are sisters to the vascular plants.

Keywords: evolution/land plants/plant cell wall/xyloglucan

Introduction

The growing cells of avascular and vascular land plants are surrounded by a cell wall composed predominantly of cellulose microfibrils embedded in a matrix of pectic and hemicellulosic polysaccharides (Ligrone et al. 2002; Popper and Fry 2003, 2004; Matsunaga et al. 2004; Niklas 2004; Carfa et al. 2005). The overall structural features of several of the polysaccharides in the cell walls of angiosperms have been established (O'Neill and York 2003). By contrast, only a limited number of studies have described the structures of polysaccharides present in the cell walls of seedless vascular (Lycopodiophytes [club and spike mosses] and Monilophytes [ferns and their allies]) and avascular plants (Marchantiophytes [liverworts], Bryophytes [mosses], and Anthocerotophytes [hornworts]) (Popper and Fry 2003, 2004; Matsunaga et al. 2004; Sørensen et al. 2008; Fry, Nesselrode et al. 2008). Nevertheless, these studies suggest that cell wall composition and structure changed when plants first adapted to life on land and during the subsequent evolutionary events that led to the appearance of vascular tissues and flowering plants (Popper 2008).

Xyloglucan (XyG) is a quantitatively major hemicellulosic polysaccharide in the primary cell walls of dicots and nongraminaeceous monocots (O'Neill and York 2003) and has been reported to be present in the walls of basal land plants (Popper and Fry 2003, 2004). Most seed-bearing plants produce an XXXG-type XyG, in which three consecutive (1→4)-linked β-D-Glc$p$ backbone residues bear sidechains. XXGG- and XXGGG-type XyGs, in which two consecutive backbone residues bear sidechains, are synthesized by some Lamiids (Hoffman et al. 2005) and by grasses (Gibeaut et al. 2004).

Xyloglucan structures are typically described using a single letter nomenclature to represent the substitution pattern of each backbone glucosyl residue (Fry et al. 1993). For example, the letters **G** and **X** denote an unbranched Glc$p$ residue and the α-D-Xyl$p$-(1→6)-β-D-Glc$p$ motif, respectively. The xylosyl residues may be substituted with a β-D-Gal$p$ (**L** sidechain), an α-L-Ara$f$ (**S** sidechain), or a β-D-Xyl$p$ residue (**U** sidechain) (Ray et al. 2004; Hoffman et al. 2005). The Gal residue of sidechain **L** is often substituted at O-2 with an α-L-Fuc$p$ residue to form the **F** sidechain (Hoffman et al. 2005). In jojoba XyG, the **L** sidechain is extended with an α-L-Gal$p$ residue to form the **J** sidechain (Hantus et al. 1997). In tomato XyG, the Ara$f$ residue of the **S** sidechain is occasionally substituted with a β-L-Ara$f$ residue to form the **T** sidechain (York et al. 1996). Virtually no data are available to describe the structures of avascular and seedless vascular plants XyGs. This lack of information is an impediment to understanding changes in XyG structure that occurred during land plant evolution and to understanding XyG function.

To further explore the relationships between XyG structure and function, we have isolated and structurally characterized XyGs from selected members of the three divisions of avascular land plants (liverworts, mosses, and hornworts) and from selected seedless vascular plants (club and spike mosses and ferns and fern allies). We show that moss and liverwort XyGs are structurally distinct from the XyGs of hornworts and

[1]To whom correspondence should be addressed: Tel: +1-706-542-4419; Fax: +1-706-542-4412; e-mail: mpena@ccrc.uga.edu
*Dedicated to the memory of Roger A. O'Neill, 1957–2008.

vascular plants. We also identify several unique sidechains in XyGs produced by Lycopodiophytes and Monilophytes. Our study provides new insight into the evolution and diversity of structural motifs in land plant XyGs and provides additional support to the proposal that hornworts are sisters to the vascular plants.

Results

Alcohol insoluble residues (AIRs) were prepared from *Physcomitrella patens* protonema and leafy gametophores and from the aerial growing tissues of the gametophyte generations of the liverwort *Marchantia polymorpha* and the hornworts *Anthoceros agrestis*, *Phaeoceros sp.*, *and Megaceros sp.* AIRs were also prepared from the gametophytic generation of the monilophyte *Ceratopteris richardii*, the sporophyte generations of the lycopodiophytes *Lycopodium tristachyum*, *Huperzia lucidulum*, and *Selaginella kraussianna*, and the sporophyte generations of the monilophytes *Equisetum hyemale*, *Psilotum nudum*, and *Platycerium bifurcatum*. In preliminary experiments we established that xyloglucan-specific endoglucanse (XEG)-susceptible material was solubilized by treating the depectinated AIRs with 4 N KOH. Based on the amount of material solubilized by 4 N KOH and the proportion of this material that was fragmented by XEG, we estimated that xyloglucan accounts for between 2 and 4% w/w of the AIR from the avascular plants and between 5 and 10% of the AIR from the vascular plants.

Mixtures of xyloglucan oligosaccharides (XyGOs) resulting from XEG treatment of the 4 N KOH-soluble materials were, unless stated otherwise, converted to their corresponding oligoglycosyl alditols (XyGols). When possible individual XyGols were isolated and structurally characterized using ^{1}H-NMR spectroscopy, matrix-assisted laser-desorption-time-of-flight mass spectrometry (MALDI-TOF-MS), electrospray-ionization mass spectrometry (ESI-MS), and by glycosyl residue and glycosyl-linkage composition analyses (see *Material and methods* and Supplemental data).

The moss Physcomitrella patens synthesizes XyGs that contain galacturonic acid

The moss *Physcomitrella* has become a model for studying many aspects of plant biology in part because of the ease with which it can be genetically modified (Schaefer and Zrÿd 2001; Huether et al. 2005; Quatrano et al. 2007). To evaluate the value of *Physcomitrella* as a model for cell wall studies, it is necessary to compare the structures of the polysaccharides present in its walls and in the walls of other plants (Lee et al. 2005).

The complexity of Physcomitrella XyG is evident in the MALDI-TOF mass spectrum of the XyGOs generated from protonema and leafy gametophores (Figure 1). Four series of ions, each composed of members that differ by 162 Da (the anhydrous mass of a hexosyl residue), are present in these spectra. The first series ([M + Na]$^+$ ions at *m/z* 953, 1115, 1277, 1439, 1601, and 1763) corresponds to XyGOs composed of four to nine hexosyl residues and two pentosyl residues. The second series ([M + Na]$^+$ ions at *m/z* 1085, 1247, 1409, 1571, 1733, and 1895) corresponds to XyGOs composed of four to nine hexosyl residues and three pentosyl residues. The third series ([M + Na]$^+$ ions at *m/z* 1291, 1453, 1615, 1777, and 1939) corresponds to XyGOs composed of five to nine hexosyl residues, two pentosyl
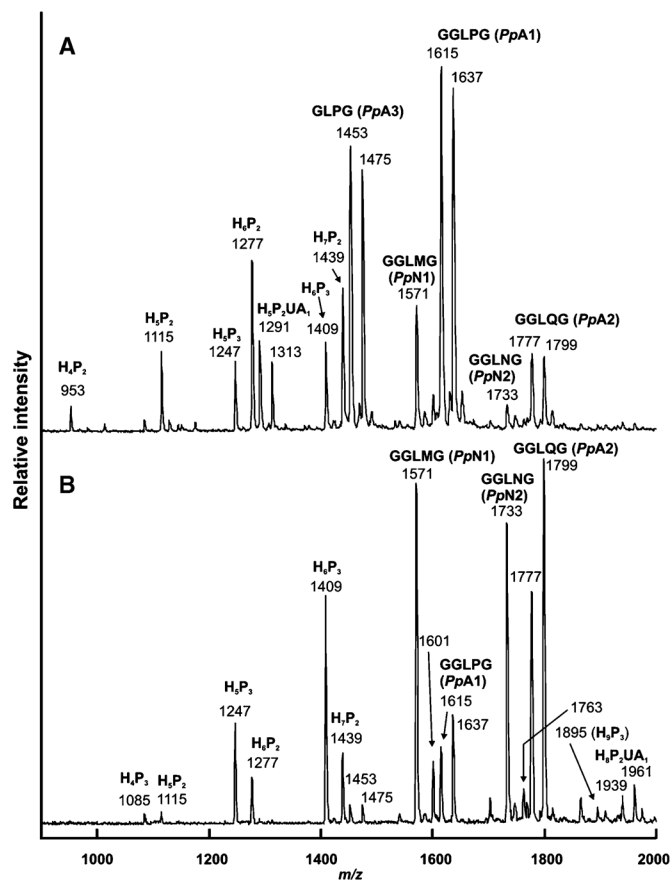
Fig. 1. MALDI-TOF mass spectra of the oligosaccharides generated by xyloglucan-specific endoglucanase treatment of Physcomitrella xyloglucan. Xyloglucan oligosaccharides were generated enzymically from xyloglucan isolated from Physcomitrella leafy gametophores (**A**) and from Physcomitrella protonema (**B**). The bold letters above each peak correspond to the subunit sequence of each oligosaccharide (see Figure 3 for details). Where the subunit structure could not be determined unambiguously we have labeled the peak with the deduced number of hexosyl (H), pentosyl (P), and hexosyluronic acid (UA) residues that are present.

residues, and a component with an anhydrous mass of 176 Da, consistent with the presence of a hexuronosyl residue. The doubly sodiated fourth series ([M − H + 2Na]$^+$ ions at *m/z* 1313, 1475, 1637, 1799, and 1961) and the singly sodiated third series have the same glycosyl compositions. The detection of doubly sodiated ions is consistent with the presence of a hexuronosyl residue.

The Physcomitrella protonema and leaf XyGOs were separately converted to their corresponding oligoglycosyl alditols (XyGols) and the neutral and acidic XyGols isolated by size-exclusion chromatography on a Sephadex G-25 column eluted with water (Peña et al. 2007). The acidic fractions were then fractionated by reversed-phase high-performance liquid chromatography (HPLC). Three acidic XyGols were isolated in amount sufficient for their complete structural characterization. Two of the acidic XyGols (*Pp*A1 [M − H + 2Na]$^+$ ion at *m/z* 1639 − deduced composition of seven hexoses, two pentoses, and one hexuronic acid and *Pp*A3 [M − H + 2Na]$^+$ ion at *m/z* 1477 − deduced composition six hexoses, two pentoses, and one hexuronic acid) were obtained from leafy gametophores and one

Table I. ^{1}H-NMR shifts (ppm) for the major acidic (**GGLPGol** and **GGLQGol**) and neutral (**GGLMGol** and **GGLNGol**) Physcomitrella XyGOLs

Residue	H-1	H-2	H-3	H-4	H-5	H-5$_{eq}$	H-6	H-6′
GGLPGol (*Pp*A1)[a]								
(**L**) t-β-Gal*p* [b]	4.547	3.627	3.661	3.921	3.680	–	3.778	3.803
(**P**) t-β-Gal*p*A	4.600	3.630	3.701	4.194	4.033	–	–	–
(**P**) t-β-Gal*p* (Xyl)[c]	4.478	3.549	3.650	3.916	3.704	–	3.742	3.815
(**L**) 2-α-Xyl*p*[d]	5.183	3.663	3.939	3.657	3.572	3.734	–	–
(**P**) 2,4-α-Xyl*p*	5.270	3.779	3.998	3.881	3.657	3.868	–	–
t-β-Glc*p*	4.507	3.309	3.507	3.415	3.484	–	3.733	3.914
4-β-Glc*p*	4.538	3.388	3.644	3.639	3.610	–	3.832	3.982
(**L**) 4,6-β-Glc*p*	4.523	3.445	3.686	3.686	3.898	–	3.97	3.938
(**P**) 4,6-β-Glc*p*	4.650	3.432	3.688	3.688	3.918	–	3.98	3.95
4-Glcol	na[e]	3.957	3.864	3.900	3.939	–	3.746	3.874
GGLQGol (*Pp*A2)								
(**Q**) t-β-Gal*p* (GalA)	4.553	3.584	3.629	3.855	3.735	–	3.756	3.801
(**L**) t-β-Gal*p*	4.547	3.629	3.661	3.922	3.680	–	3.778	3.803
(**Q**) 4-β-Gal*p*A	4.639	3.732	3.801	4.405	4.037	–	–	–
(**Q**) t-β-Gal*p* (Xyl)	4.474	3.545	3.650	3.916	3.704	–	3.742	3.815
(**L**) 2-α-Xyl*p*	5.180	3.664	3.932	3.659	3.574	3.736	–	–
(**Q**) 2,4-α-Xyl*p*	5.227	3.803	4.014	3.884	3.651	3.875	–	–
t-β-Glc*p*	4.506	3.311	3.505	3.413	3.486	–	3.734	3.913
4-β-Glc*p*	4.535	3.383	3.644	3.639	3.610	–	3.832	3.982
(**L**) 4,6-β-Glc*p*	4.518	3.452	3.690	3.688	3.904	–	3.97	3.938
(**Q**) 4,6-β-Glc*p*	4.657	3.431	3.702	3.679	3.923	–	3.98	3.95
4-Glcol	na	na	na	na	3.972	–	3.753	3.871
GGLMGol (*Pp*N1)								
(**L**) t-β-Gal*p*	4.551	3.627	3.661	3.922	3.680	–	3.778	3.803
(**M**) t-α-Ara*p*	4.503	3.644	3.671	3.934	3.684	3.789	–	–
(**M**) t-β-Gal*p* (Xyl)	4.476	3.545	3.644	3.917	3.704	–	3.742	3.815
(**L**) 2-α-Xyl*p*	5.180	3.667	3.920	3.666	3.575	3.732	–	–
(**M**) 2,4-α-Xyl*p*	5.134	3.694	3.978	3.882	3.651	3.875	–	–
t-β-Glc*p*	4.503	3.311	3.501	3.412	3.485	–	3.734	3.914
4-β-Glc*p*	4.542	3.385	3.644	3.639	3.619	–	3.832	3.986
(**L**) 4,6-β-Glc*p*	4.556	3.423	3.688	3.688	3.888	–	3.987	3.943
(**M**) 4,6-β-Glc*p*	4.613	3.445	3.667	3.679	3.921	–	3.9	3.9
4-Glcol	na	na	na	na	3.972	–	3.753	3.871
GGLNGol (*Pp*N2)								
(**N**) t-β-Gal*p* (Gal)	4.516	3.539	3.672	3.925	na	–	na	na
(**L**) t-β-Gal*p*	4.551	3.626	3.661	3.920	3.650	–	3.778	3.803
(**N**) t-α-Ara*p*	4.507	3.645	3.695	3.934	3.691	3.787	–	–
(**N**) 6-β-Gal*p* (Xyl)	4.486	3.558	3.661	3.956	3.924	–	4.053	3.957
(**L**) 2-α-Xyl*p*	5.185	3.669	3.921	3.663	3.574	3.737	–	–
(**N**) 2,4-α-Xyl*p*	5.137	3.704	3.975	3.883	3.657	3.907	–	–
t-β-Glc*p*	4.505	3.311	3.504	3.414	3.485	–	3.732	3.913
4-β-Glc*p*	4.542	3.389	3.645	3.639	3.619	–	3.830	3.986
(**L**) 4,6-β-Glc*p*	4.551	3.425	3.691	3.688	3.884	–	3.987	3.943
(**N**) 4,6-β-Glc*p*	4.614	3.445	3.667	3.737	3.921	–	3.9	3.9
4-Glcol	na	na	na	na	3.961	–	3.751	3.871

[a]See Figure 3 for the structures of the oligosaccharides.
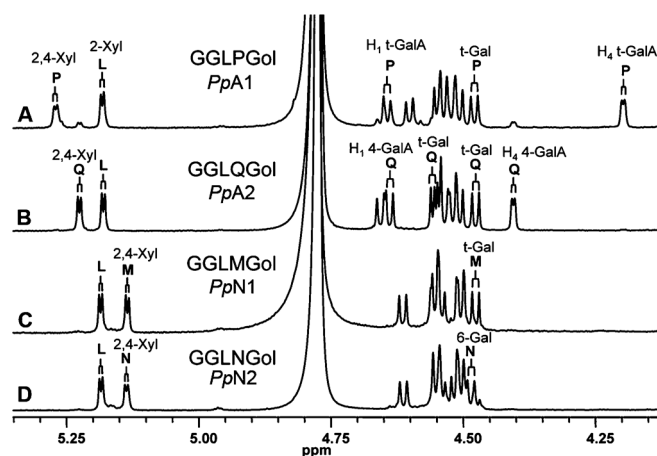[b](**L**) t-β-Gal*p* is terminal β-linked galactose in sidechain **L**, etc.
[c]The glycose in parenthesis is the glycose to which the Gal*p* is linked.
[d]Only Ara*p* and Xyl*p* have H-5$_{ax}$ and H-5$_{eq}$.
[e]na, resonances not assigned.

Fig. 2. Partial 600-MHz ^{1}H-NMR spectra of Physcomitrella xyloglucan oligosaccharides **GGLPGol**, **GGLQGol**, **GGLMGol**, and **GGLNGol**. **GGLPGol** (**A**) and **GGLQGol** (**B**) are the quantitatively major acidic oligosaccharides obtained from Physcomitrella leafy gametophores and protonema xyloglucan, respectively. **GGLMGol** (**C**) and **GGLNGol** (**D**) are the quantitatively major neutral oligosaccharides obtained from Physcomitrella protonema xyloglucan. The residues corresponding to each group of proton resonances (e.g., 2,4-Xyl) are indicated at the top of each spectrum. The location of each of these residues in particular sidechains (**L**, **P**, **G**, etc.) is indicated. (See *Results* for sidechain nomenclature.)

(*Pp*A2 [M – H + 2Na]$^+$ ion at *m/z* 1801 – deduced composition of eight hexoses, two pentoses, and one hexuronic acid) from protonema.

Resonances diagnostic for the XyGol backbone and the **L** sidechain (http://cell.ccrc.uga.edu/world/xgnmr/) were present in the ^{1}H-NMR spectra of *Pp*A1, *Pp*A2, and *Pp*A3 (Table I; Figure 2). Two-dimensional NMR analyses of *Pp*A1 revealed an isolated spin system with a scalar coupling pattern that allowed it to be unambiguously assigned as a nonreducing terminal β-Gal*p*A residue (Table I). An interglycosidic NOE indicated that the Gal*p*A was linked to O-2 of an α-Xyl*p* residue that itself is substituted at O-4 with a glycosyl residue that was identified as β-Gal*p* from its unique spin system and its scalar coupling topology (Table II). The presence of terminal Gal*p*A (identified as its 6,6-dideuteriogalactosyl derivative), 2,4-linked Xyl*p*, and terminal Gal*p* residues was confirmed by glycosyl-linkage composition analysis of carboxyl-reduced *Pp*A1. All glycosyl residues in *Pp*A1 were shown to have the D-configuration by ^{1}H-NMR spectroscopic analysis of the chiral per-*O*-(*S*)-2-methylbutyrate derivatives (York et al. 1997). Together, these results led us to conclude that *Pp*A1 has a unique, branched sidechain, to which we assign the letter **P** (see Figure 3).

A comparison of the 1D and 2D ^{1}H-NMR spectra of *Pp*A2 and *Pp*A1 showed that both contain a sidechain with 2,4-linked Xyl*p* and a β-D-Gal*p*A residue (Table I, Figure 2). These analyses also revealed the presence in *Pp*A2 of an additional spin system, identified as a β-Gal*p* residue. An NOE crosspeak indicated that this Gal*p* residue is linked to O-4 of the β-D-Gal*p*A residue (Table II), a result that is consistent with the downfield shift of several of the β-D-Gal*p*A resonances relative to those of the terminal Gal*p*A residue in *Pp*A1 (Figure 2). Glycosyl-linkage composition analysis of carboxyl-reduced *Pp*A2, confirmed the presence of 2,4-linked Xyl*p*, terminal Gal*p*, and 4-linked Gal*p*A residues. This extended sidechain was assigned the letter **Q** (see Figure 3).

The locations of unbranched β-D-Glc residues and the **L**, **P**, and **Q** sidechains in *Pp*A1 and *Pp*A2 were unambiguously determined by ESI-MS-MS analyses of their carboxyl-reduced and per-*O*-methylated derivatives. Fragment ions containing the 6,6-dideuteriogalactosyl residue (derived by carboxyl-reduction of the Gal*p*A residue) were identified by characteristic mass differences of two Da associated with dideuteration. The results were consistent with the attachment of sidechains **P** or **Q** to the Glc*p* residue adjacent to the alditol and the attachment of sidechain **L** to the adjacent 4-linked Glc residue. We conclude that *Pp*A1

Table II. NOESY cross-peaks due to dipolar interactions within the acidic (**GGLPGol** and **GGLQGol**) and neutral (**GGLMGol** and **GGLNGol**) Physcomitrella XyGOLs

	¹H resonance				Interacting ¹H resonances					
GGLPGol(*Pp*A1)ᵃ										
(**L**) t-Galp^{b,c}	H-1	4.547	→	Xylp	H-2	3.663	Xylp	H-1	5.18	
(**P**) t-GalpA	H-1	4.600	→	Xylp	H-2	3.779				
(**P**) t-Galp (Xyl)	H-1	4.478	→	Xylp	H-4	3.881				
(**L**) 2-Xylp	H-1	5.183	→	Glcp	H-6	3.93				
(**P**) 2,4-Xylp	H-1	5.270	→	Glcp	H-6	3.9				
GGLQGol(*Pp*A2)										
(**Q**) t-Galp (GalA)	H-1	4.553	→	GalpA	H-4	4.405				
(**L**) t-Galp^c	H-1	4.547	→	Xylp	H-2	3.664	Xylp	H-1	5.18	
(**Q**) 4-GalpA	H-1	4.639	→	Xylp	H-2	3.803				
(**Q**) t-Galp (Xyl)	H-1	4.474	→	Xylp	H-4	3.884				
(**L**) 2-Xylp	H-1	5.180	→	Glcp	H-6	3.93				
(**Q**) 2,4-Xylp	H-1	5.227	→	Glcp	H-6	3.9				
GGLMGol(*Pp*N1)										
(**L**) t-Galp^c	H-1	4.551	→	Xylp	H-2	3.667	Xylp	H-1	5.18	
(**M**) t-Arap	H-1	4.503	→	Xylp	H-2	3.694				
(**M**) t-Galp (Xyl)	H-1	4.476	→	Xylp	H-4	3.882				
(**L**) 2-Xylp	H-1	5.180	→	Glcp	H-6	3.94				
(**M**) 2,4-Xylp	H-1	5.131	→	Glcp	H-6	3.9				
GGLNGol(*Pp*N2)										
(**L**) t-Galp^c	H-1	4.551	→	Xylp	H-2	3.669	Xylp	H-1	5.18	
(**N**) t-Arap	H-1	4.507	→	Xylp	H-2	3.404				
(**N**) t-Galp (Xyl)	H-1	4.486	→	Xylp	H-4	3.883				
(**L**) 2-Xylp	H-1	5.185	→	Glcp	H-6	3.94				
(**N**) 2,4-Xylp	H-1	5.137	→	Glcp	H-6	3.9				

ᵃSee Figure 3 for details of oligosaccharide structures.
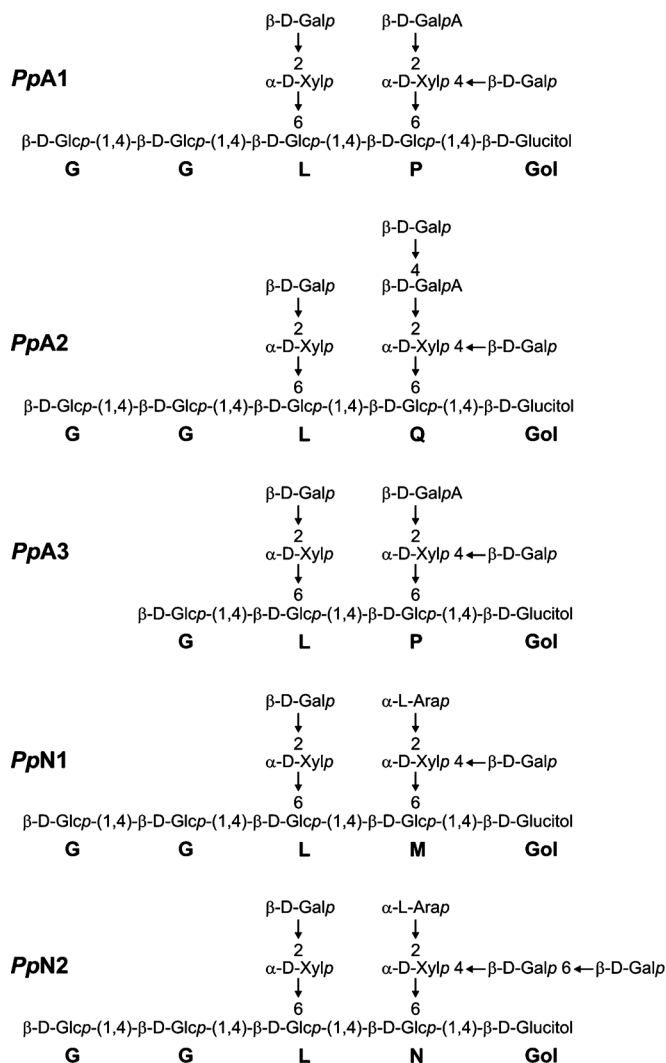ᵇ(**L**) t-Galp is the terminal no-reducing galactosyl residue in sidechain **L** etc.
ᶜH-1 of the t-Galp interacts with H-1 and H-2 of the Xylp residue.

Fig. 3. Glycosyl sequences of the major acidic (**GGLPGol**, **GGLQGol**, and **GLPGol**) and neutral (**GGLMGol** and **GGLNGol**) oligosaccharides generated from Physcomitrella xyloglucan. All oligosaccharides were structurally characterized as their oligosaccharide alditols.

and *Pp*A2 have the sequences **GGLPGol** and **GGLQGol**, respectively (Figure 3).

¹H-NMR analyses established that *Pp*A3 also contained sidechain **P**. However, *Pp*A3 (**GLPGol**) has one less glucosyl residue in its backbone than *Pp*A1 (**GGLPGol**). This difference is likely due to the fact that the XEG used in this study can hydrolyze the sequence **GGXXGGGLPG** at two different sites, leading to the production of **GGXXG** and **GGLPG** or **GGXXGG** and **GLPG**. The XEG does not efficiently cleave the glycosidic bond between **G** and **X** to generate **XXG** oligosaccharides when there are three consecutive unsubstituted **G**s (Jia et al. 2003). Together these results indicate that Physcomitrella XyG has an XXGGG-type branching pattern.

Two Physcomitrella neutral XyGOls (*Pp*N1 [M + Na]⁺ ion at *m/z* 1573 – deduced composition of seven hexoses and three pentoses and *Pp*N2 [M + Na]⁺ ion at *m/z* 1735 – deduced composition of eight hexoses and three pentoses) were obtained from protonema in amounts sufficient for their structural characterization. Several other XyGOs are generated in small amounts by XEG treatment of Physcomitrella XyG (see Figure 1). ¹H-NMR analysis suggests that some of these XyGOs contain the **X** sidechain but further analysis is required for their full characterization.

The 2D ¹H-NMR spectra of *Pp*N1 and *Pp*N2 contained resonances within an isolated spin system having chemical shifts and coupling pattern (Table I) characteristic of an α-linked arabinopyranosyl residue (Glushka et al. 2003). This is the first report of an Arap residue in a XyG and was unexpected, as all previously identified arabinosyl residues in XyGs exist in the furanosyl form. 2D ¹H-NMR analysis of *Pp*N1 indicated that this α-Arap residue is linked to O-2 of a 2,4-linked α-Xylp residue (Table I) and that a β-Galp residue is linked to O-4 of this branched α-Xylp residue (Table II). Glycosyl-linkage analysis confirmed that *Pp*N1 contains 2,4-linked Xylp, terminal Arap, and terminal Galp residues. These results, in combination with data establishing that the arabinose is ʟ and all other glycoses are ᴅ, indicate that *Pp*N1 contains a sidechain to which we assign the letter **M**. **M** is structurally homologous to sidechain **P**, except that the β-ᴅ-GalpA residue is replaced by an α-ʟ-Arap residue (see Figure 3).

*Pp*N2 and *Pp*N1 are structurally homologous, except that *Pp*N2 contains an additional hexosyl residue. ¹H-NMR analysis identified this additional residue as a terminal β-Galp that is attached to another β-Gal, which itself is linked to O-4 of the 2,4-linked Xylp (Tables I and II; Figure 2). Glycosyl-linkage composition analysis confirmed the presence of terminal and 6-linked Galp and terminal Arap residues. Again the Ara is ʟ

894

and all other glycoses are D. These results together indicate a sidechain, to which we assign the letter **N**, in which the xylosyl residue is substituted at O-2 with α-L-Ara*p* and at O-4 with β-D-Gal*p*-(1,6)-β-D-Gal*p* (Figure 3). The locations of sidechains **L**, **M**, and **N** along the XyGol backbone were determined by ^{1}H-NMR, establishing the sequences **GGLMGol** for *Pp***N1** and **GGLNGol** for *Pp***N2** (Figure 3).

We conclude that Physcomitrella XyG has an XXGGG-type branching pattern and is thus similar to the XyGs synthesized by certain members of the Lamiales (Hoffman et al. 2005). However, the sidechains of Physcomitrella XyG are structurally distinct from those synthesized by the Lamiales and by all other vascular plants.

The liverwort *Marchantia polymorpha* synthesizes XyGs that contain galacturonic acid

To determine whether Gal*p*A was a component of liverwort XyG, XyG was isolated from the walls of *M. polymorpha*. MALDI-TOF-MS and ^{1}H-NMR analyses of the XyGols indicated that this XyG has an XXGG-type branching pattern and is composed predominantly of subunits bearing **X** and **L** sidechains. The 2D ^{1}H-NMR spectra contained signals consistent with the presence of β-Gal*p*A and branched α-Xyl*p* residues in sidechain **P**. Some of the sidechain **P** resonances in the liverwort XyGols and in *Pp***A1** (**GGLPGol**) have chemical shifts that are not identical. We attribute these differences to the fact that Marchantia and Physcomitrella XyGs have different sidechain compositions. Indeed, MALDI-TOF-MS indicated that the Marchantia subunits contain fewer hexosyl residues than the Physcomitrella subunits. Moreover, the absence of signals for α-L-Ara*p* residues in the ^{1}H-NMR spectra indicated that liverwort XyG contains no **M** and **N** sidechains. However, the ^{1}H-NMR spectra did indicate the presence of trace amounts of sidechain **Q**. Chemical shift differences for the **P** sidechain in **GGXPGol** and **GGLPGol** are thus likely due to the proximity of an **X** sidechain rather than an **L** sidechain.

Hornworts synthesize XyGs that are structurally homologous to XyGs of seed-bearing plants

Having established that *Physcomitrella* and *Marchantia* synthesize XyGs that contain Gal*p*A and branched Xyl*p* residues, we isolated XyG from three different hornworts to determine if these features are general characteristics of avascular plant XyGs. Somewhat unexpectedly, all three hornworts synthesized XyG that is structurally homologous to the XyG synthesized by many seed-bearing plants. MALDI-TOF-MS analysis (Figure 4) of the XyGOs generated from Anthoceros and Phaeoceros XyG indicated that these XyGs have an XXXG-type branching pattern with **XXXG**, **XXLG/XLXG**, **XLLG**, **XXFG**, and **XLFG** subunits. A comparison of the 2D ^{1}H-NMR spectra of the Anthoceros XyGOs and well-characterized standard XyGOs from diverse plants (York et al. 1990; Hoffman et al. 2005) allowed us to identify sidechains **X**, **L**, and **F**. Megaceros XyG is composed predominantly of **XXXG** and **XXLG/XLXG** subunits with few fucosylated oligosaccharide subunits (Figure 4). None of the distinctive structural features of Physcomitrella XyG, including the presence of Gal*p*A and branched Xyl*p* residues, were detected in the XyG of any of the hornworts analyzed.
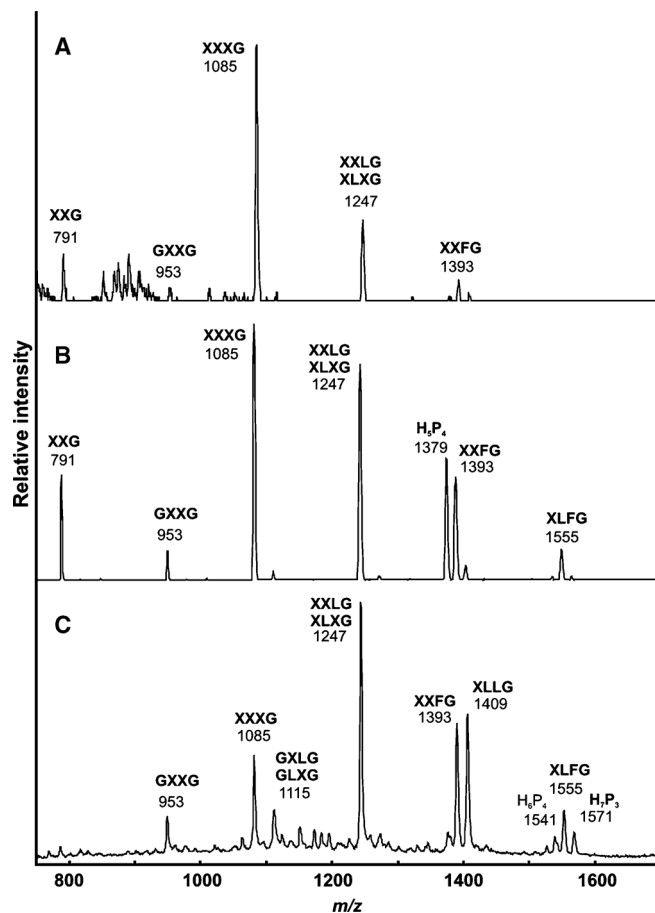
Fig. 4. MALDI-TOF mass spectra of the oligosaccharides generated by XEG-treatment of hornwort xyloglucans. Xyloglucan oligosaccharides were generated enzymatically from xyloglucan isolated from Megaceros sp. (**A**), Phaeoceros sp. (**B**), and A. agrestis (**C**) xyloglucans. The bold letters above each peak correspond to the subunit sequence of each oligosaccharide. Where the subunit could not be determined unambiguously we have labeled the peak with the deduced number of hexosyl (H) and pentosyl (P) residues that are present.

Fucosylation and branching patterns are generally conserved in the xyloglucans produced by diverse seed-bearing and seedless vascular plants

To evaluate the changes in XyG structure that may have accompanied the emergence of vascular plants, we characterized XyGs from selected lycopodiophytes and monilophytes.

MALDI-TOF-MS and ^{1}H-NMR spectroscopic analyses of the nonreduced XyGOs from the horsetail *E. hyemale* XyG established that this XyG has an XXXG-type branching pattern. Several of the XyGOs (**XXXG**, **XXLG/XLXG**, **XLLG**, and **XXFG**, see Table III) had previously been identified in XyGs from angiosperms and gymnosperms (Hoffman et al. 2005). In addition, two abundant and previously unidentified XyGOs (*Eh***1** ([M + Na]+ ion at *m/z* 1379 – deduced composition of five hexoses and four pentoses) and *Eh***2** ([M + Na]+ ion at *m/z* 1525 – deduced composition of five hexoses, four pentoses, and one deoxyhexose) were present (Table III). Glycosyl-residue composition analysis showed that *Eh***1** and *Eh***2** contained arabinose and that in *Eh***2** the deoxyhexose was Fuc. *Eh***2** was immediately

Table III. Subunit compositions of selected seed-less vascular plant XyGs deduced by MALDI-TOF-MS analyses of the XEG-generated XGOs

m/z[a]	*E. hyemale*	*C. richardii*	*P. bifurcatum*	*P. nudum*	*S. kraussiana*
			Deduced subunit composition[b]		
791	nd[c]	GXG (1)	nd	GXG (8)	nd
953	nd	GXXG (3)	nd	GXXG (7)	nd
1085	XXXG (4)	XXXG (24)	XXXG (18)	XXXG (16)	XXXG (1)
1115	nd	GXLG (2)	nd	GXLG (5)	nd
1217	XXDG (9)	XXSG (14)	nd	nd	XXDG (17)
1247	XXLG/XLXG (13)	XXLG/XLXG (15)	XXLG/XLXG (15)	XXLG/XLXG (13)	XXLG/XLXG (1)
1349	XDDG (1)	nd	nd	nd	XDDG (57)
1363	XXEG (3)	nd	nd	nd	XXEG (7)
1379	XLDG (43)	XLSG (22)	nd	nd	XLDG (7)
1393	XXFG (2)	XXFG (7)	XXFG (15)	XXFG (19)	XXFG (7)
1409	XLLG (2)	XLLG (9)	XLLG (11)	XLLG (6)	XLLG (1)
1495	XDEG (tr)	nd	nd	nd	XDEG (3)
1525	XLEG (22)	nd	nd	nd	XLEG (4)
1555	XLFG(1)	XLFG (3)	XLFG (41)	XLFG (25)	XLFG (1)

[a] the $[M + Na]^+$ ion.
[b] The values in parenthesis are the relative abundance of each subunit.
[c] nd, not detected.
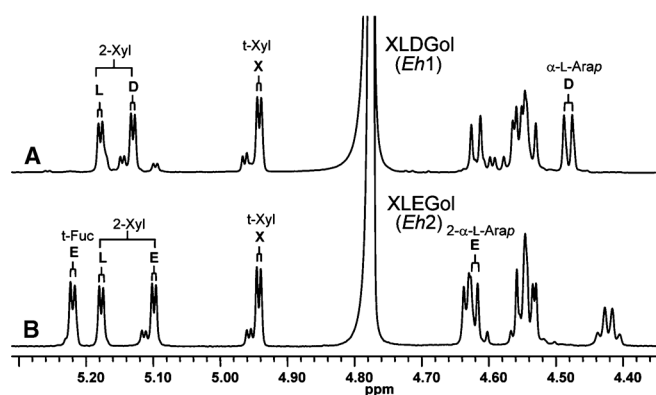
Fig. 5. Anomeric regions of the 1D ^{1}H-NMR spectra of the **XLDGol** (**A**) and **XLEGol** (**B**) generated from *E. hyemale* xyloglucan. The residues corresponding to each group of anomeric proton resonances are indicated at the top of the figure. The location of each of these residues in specific sidechains (**X**, **L**, **D**, or **E**) is indicated below the brackets. (See *Results* and Figure 6 for sidechain nomenclature.)

recognized as a unique structure, as no XyGO containing both fucose and arabinose had previously been identified.

*Eh*1 and *Eh*2 were converted to their corresponding oligoglycosyl alditols, isolated and then characterized by ^{1}H-NMR spectroscopy (Figure 5; Table IV). *Eh*1 contains an **X** sidechain at the nonreducing end of the XyGol backbone and an **L** sidechain at another position. We also observed a residue with a spin topology characteristic of the terminal α-Ara*p* previously identified in the **M** and **N** sidechains. Chemical shift effects (Table IV) indicated that the α-Ara*p* residue is linked to O-2 of an α-Xyl*p* residue. Glycosyl-linkage composition analysis confirmed the presence of terminal Xyl*p*, terminal Ara*p*, and 2-linked Xyl*p* residues. These results, in combination with data showing that the Ara is L and all other glycoses D, established the presence of an α-L-Ara*p*-(1→2)-α-D-Xyl*p*- sidechain, to which we assign the letter **D**. We conclude that *Eh*1 has the sequence **XLDGol**

(Figure 6). ^{1}H-NMR spectroscopic analysis (Figure 5) also indicated the presence of two additional low-abundance oligosaccharides. One contained an α-Ara*p* residue and was assigned the sequence **XXDGol**, whereas the second contained an α-Ara*f* residue and was assigned the tentative sequence **XXSGol**.

Our 2D ^{1}H-NMR data (Figure 5 and Table IV) established that in *Eh*2 the α-Fuc*p* residue is linked to O-2 of an α-Ara*p* residue and that *Eh*2 also contain sidechain **L**. Glycosyl-linkage composition analysis confirmed the presence of terminal Fuc*p*, 2-linked Ara*p*, 2-linked Xyl*p*, and terminal Gal*p* residues. The Ara and Fuc are L and all other glycoses D. The combined results indicate that *Eh*2 contains the unique sidechain α-L-Fuc*p*-(1→2)-α-L-Ara*p*-(1→2)-α-D-Xyl*p*-, to which we assign the letter **E** (Figure 6) and allowed us to assign the sequence **XLEGol** to *Eh*2. The presence of additional low-abundance resonances in the ^{1}H-NMR spectrum of *Eh*2 was attributed to the presence of **XXEGol**.

Xyloglucans isolated from the ferns *C. richardii* and *P. bifurcatum* and the fern ally *P. nudum* were also characterized. MALDI-TOF-MS (Table III) of the nonreduced XyGOs indicated that *P. bifurcatum* and *P. nudum* synthesize XXXG-type XyGs composed of subunits (**XXXG, XLXL/XXLG, XXFG, XLLG,** and **XLFG**) that are also found in many seed-bearing plant XyGs. MALDI-TOF-MS analysis together with 1D and 2D ^{1}H-NMR spectroscopic analyses (data not shown) indicated that the *C. richardii* XyGOs contained **S** as well as **X**, **L**, and **F** sidechains and established that *C. richardii* XyG has an XXXG-type branching pattern with **XXXG, XXSG/XSXG, XXLG/XLXG, XLSG, XLLG,** and **XXFG** subunits (Table III). This combination of subunits is also present in the XyG produced by *Nerium oleander*, a Lamiid in the order Gentianales (Hoffman et al. 2005).

^{1}H-NMR analysis of XyGOs generated from the XyG of the lycopodiophytye *S. kraussiana* showed that it is similar but not identical to the XyG produced by *E. hyemale*. Both XyGs have an XXXG-type branching pattern, although the Selaginella XyG is more highly substituted with α-L-Ara*p* residues. Our ^{1}H-NMR analyses and MALDI-TOF-MS analysis of the nonreduced

Table IV. ^{1}H-NMR shifts (ppm) and NOE connectivities for **XLDGol** and **XLEGol** generated from *E. hemale* XyG

Residue	H-1	H-2	H-3	H-4	H-5	H-5$_e$	H-6	H-6′					
XLDGol(*Eh*1)[a]													
(**L**) t-β−Gal*p*[b]	4.553	3.621	3.662	3.921	3.682	–	3.759	3.803			NOE connectivities		
(**D**) t-α-Ara*p*	4.482	3.636	3.665	3.934	3.680	3.772	–	–					
(**X**) t-α-Xyl*p*	4.943	3.541	3.734	3.613	3.544	3.713	–	–	(**X**) Xyl*p* H-1	4.94	→	Glc*p* H-6	3.78
(**L**) 2-α-Xyl*p*	5.178	3.669	3.923	3.667	3.544	3.733	–	–	(**L**) Xyl*p* H-1	5.17	→	Glc*p* H-6	3.96
(**D**) 2-α-Xyl*p*	5.130	3.636	3.836	3.672	3.580	3.728	–	–	(**D**) Xyl*p* H-1	5.13	→	Glc*p* H-6	3.93
(**X**) t-β-Glc*p*	4.538	3.339	3.513	3.527	3.696	–	3.780	3.943					
(**L**) t-β-Glc*p*	4.558	3.416	3.667	3.667	3.897	–	3.964	3.928					
(**D**) t-β-Glc*p*	4.620	3.444	3.672	3.677	3.820	–	3.938	3.907					
4-Glcol	3.775	3.936	3.918	3.940	3.962	–	3.746	3.867					
											NOE connectivities		
XLEGol (*Eh*2)													
(**E**) t-α-Fuc*p*	5.220	3.793	3.880	3.806	4.420	–	1.247	–	(**E**) Fuc*p* H-1	5.22	→	Ara*p* H-2	3.77
(**L**) t-β-Gal*p*	4.551	3.618	3.662	3.921	3.681	–	3.760	3.804					
(**E**) t-α-Ara*p*	4.630	3.779	3.905	3.951	3.629	3.918	–	–	(**E**) Ara*p* H-1	4.63	→	Xyl*p* H-2	3.61
(**X**) t-α-Xyl*p*	4.943	3.542	3.733	3.613	3.544	3.711	–	–	(**X**) Xyl*p* H-1	4.94	→	Glc*p* H-6	3.78
(**L**) 2-α-Xyl*p*	5.176	3.670	3.922	3.633	3.544	3.733	–	–	(**L**) Xyl*p* H-1	5.17	→	Glc*p* H-6	3.96
(**E**) 2-α-Xyl*p*	5.100	3.612	3.785	3.669	3.576	3.723	–	–	(**E**) Xyl*p* H-1	5.10	→	Glc*p* H-6	3.9
(**X**) t-β-Glc*p*	4.535	3.337	3.516	3.527	3.696	–	3.783	3.941					
(**L**) t-β-Glc*p*	4.540	3.421	3.668	3.667	3.897	–	3.964	3.928					
(**E**) t-β-Glc*p*	4.622	3.432	3.685	3.679	3.855	–	3.9	3.9					
4-Glcol	na[c]	na	na	3.899	3.056	–	3.752	3.855					

[a]See Figure 6 for oligosaccharide structures.
[b](**L**) t-β-Gal*p* is terminal β-linked galactose in sidechain L, etc.
[c]na, not assigned.

XyGOs (Table III) established that **XDDG** is the most abundant subunit of the Selaginella XyG and that this XyG also contains all of the oligosaccharide subunits identified in Equisetum XyG, including **XDEG** (Table III).

The lycopodiophytes *L. tristachyum* and *H. lucidula* produce structurally complex XyGs, which we only partially characterized. Mono-*O*-methylated glycosyl residues, including 3-*O*-methyl D-Gal, were detected by ^{1}H-NMR and identified by glycosyl residue composition analysis and contribute to the complexity of the XyGs from these lycopodiophytes. *O*-Methylated sugars have previously been reported to be components of the cell walls of lycopodiophytyes (Popper et al. 2001). MALDI-TOF-MS analysis of the lycopodiophytye XyGols suggests that these plants produce XyGs in which the XXGG-type branching pattern predominates. However, our data do not preclude the possibility that XXXG-type branching patterns are also present. A comparison of the ^{1}H-NMR spectra of the lycopohyte Xy-Gols to those of well-characterized XyGols from seed-bearing plants (http://cell.ccrc.uga.edu/world/xgnmr/) and from Equisetum (this manuscript) indicated that sidechains **X**, **L**, and **D** are abundant. The XyG of *L. tristachyum* also contained small amounts of the **E** and **F** sidechains.
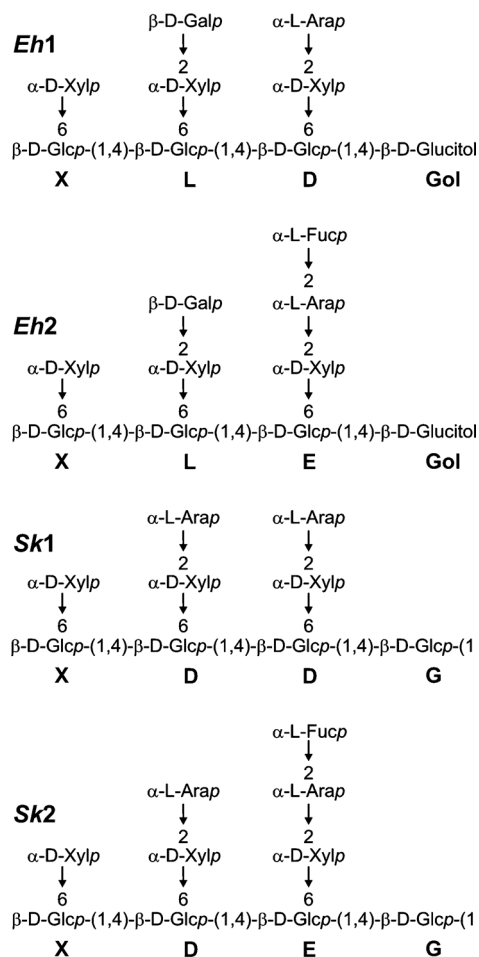
Discussion

Our study provides compelling evidence that XyG is present in the cell walls of all land plants. Seedless vascular plants and the avascular hornworts synthesize XyGs that are structural homologs of the XyGs produced by seed-bearing plants. By contrast, the XyGs synthesized by mosses and liverworts are unique as some of their sidechains contain a β-linked galactosyluronic acid residue and a branched xylosyl residue.

Xyloglucan structure and the phylogenetic relationships of avascular and vascular plants

Recent studies of land plant phylogeny place hornworts as sister to the vascular plants (Qiu et al. 2006). Our data are consistent with this notion as hornworts are the only avascular plants in which we detected XXXG-type XyGs with fucosylated subunits. This combination of structural motifs is likely to be a common characteristic of hornworts, as we characterized XyGs from three different hornworts (Anthoceros, Phaeoceros, and Megaceros, see Figure 4), which account for approximately 1% of the named species in the phylum Anthocerotophyta (Duff et al. 2007). We suggest that fucogalactosyl XyG first appeared in a common ancestor of hornworts and vascular plants (Figure 7) and then became a common characteristic of the XyGs synthesized by many vascular plants (Table III; Hoffman et al. 2005).

The unique acidic XyG of the moss Physcomitrella and the liverwort Marchantia

Our data suggest that mosses and liverworts are the only land plants that synthesize XyGs that contain a 2,4-linked α-D-Xyl*p* residue (sidechains **M**, **N**, **P**, and **Q**, see Figure 3). Two of these sidechains (**P** and **Q**) also contain a β-D-Gal*p*A residue, which is unusual as the vast majority of Gal*p*A residues are α-linked in the cell wall polysaccharides of Embryophytes. Furthermore, no galactosyluronic-acid-containing sidechains have been identified in the XyGs produced by any vascular plant. Angiosperm XyGs have been reported to behave like polyanions (Thompson and Fry 2000), although there is no evidence that these XyGs contain acidic sugars. Rather, it is likely that their anionic behavior is due to a close association with pectic polysaccharides (Popper and Fry 2005).

Eh1

```
                    β-D-Galp          α-L-Arap
                      ↓2                ↓2
   α-D-Xylp        α-D-Xylp          α-D-Xylp
      ↓6              ↓6                ↓6
β-D-Glcp-(1,4)-β-D-Glcp-(1,4)-β-D-Glcp-(1,4)-β-D-Glucitol
      X               L                 D               Gol
```

Eh2

```
                                      α-L-Fucp
                                        ↓2
                    β-D-Galp          α-L-Arap
                      ↓2                ↓2
   α-D-Xylp        α-D-Xylp          α-D-Xylp
      ↓6              ↓6                ↓6
β-D-Glcp-(1,4)-β-D-Glcp-(1,4)-β-D-Glcp-(1,4)-β-D-Glucitol
      X               L                 E               Gol
```

Sk1

```
                    α-L-Arap          α-L-Arap
                      ↓2                ↓2
   α-D-Xylp        α-D-Xylp          α-D-Xylp
      ↓6              ↓6                ↓6
β-D-Glcp-(1,4)-β-D-Glcp-(1,4)-β-D-Glcp-(1,4)-β-D-Glcp-(1
      X               D                 D               G
```

Sk2

```
                                      α-L-Fucp
                                        ↓2
                    α-L-Arap          α-L-Arap
                      ↓2                ↓2
   α-D-Xylp        α-D-Xylp          α-D-Xylp
      ↓6              ↓6                ↓6
β-D-Glcp-(1,4)-β-D-Glcp-(1,4)-β-D-Glcp-(1,4)-β-D-Glcp-(1
      X               D                 E               G
```

Fig. 6. Glycosyl sequences of the major oligosaccharide subunits of *E. hyemale* and *S. kraussiana* xyloglucans. The Equisetum XyGOs **XLDGol** and **XLEGol** were structurally characterized as the oligosaccharide alditols. The Selaginella XyGOs **XDDG** and **XDEG** were structurally characterized as the reducing oligosaccharides.

Interestingly, we found that the ratios of **GGLQG** to **GGLPG** and **GGLNG** to **GGLMG** are significantly higher in protonema XyG than in leafy gametophore XyG (see Figure 1). Thus, in protonema XyG extension of the branched sidechains with Galp residues is more pronounced. Specific structural features of XyG including the number of terminal Galp residues and subunit composition have been reported to be correlated with tissue type and developmental state (Pauly et al. 1999). Changes in the Physcomitrella XyG structure may also be associated with the mechanism of cell growth since protonema extend by tip growth whereas leafy gametophore cells exhibit expansive growth (Schaefer and Zrÿd 2001). Physcomitrella provides the opportunity to investigate the relationship between XyG structure and different growth mechanisms as it is now possible to selectively alter the expression of genes that encode proteins involved in XyG biosynthesis in this plant.

The fucogalactosyl structural motif is conserved in land plant xyloglucans
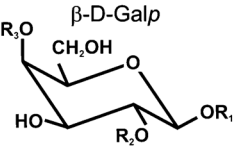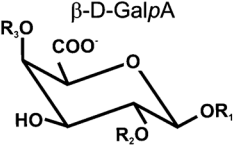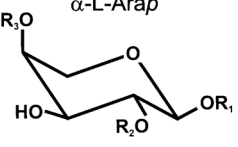
Fucosylated XyGs occur in diverse nonflowering (Table III) and flowering plants (Hoffman et al. 2005) showing that the ability to synthesize such structures has been conserved during land plant evolution. Nevertheless, the role of fucosyl residues in the biological function of XyGs remains unclear (Zablackis et al. 1996; Vanzin et al. 2002). The Arabidopsis *mur*2 and *fut*1 mutants produce XyG that lacks Fuc residues but have no visible phenotypes when grown under controlled conditions (Vanzin et al. 2002; Perrin et al. 2003). Such results are common as gene inactivation in Arabidopsis often results in plants with no visible phenotype (Bouche and Bouchez 2001). We propose that XyG fucosylation has a function that is not readily discernible in laboratory grown plants.

In many plants, the fucosyl residue is linked to O-2 of a β-D-Galp residue (**F** sidechain). By contrast, Equisetum and Selaginella XyG contain a fucosyl residue linked to O-2 of an α-L-Arap residue (**E** sidechain in **Eh1** and **Sk1**, see Figure 6). An α-L-Arap residue differs from a β-D-Galp residue only by the absence of a C-6 hydroxymethyl group

	Branching Pattern			Side chain												O-Me Sugars
	XXXG	XXGG	XXGGG	X	L	F	S	T	U	D	E	P	Q	M	N	
Seed Plants	+	+	+	+	+	+	+	+	+							
Ceratopteris	+			+	+	+	+									
Platycerium	+			+	+	+										
Psilotum	+			+	+	+										
Equisetum	+			+	+	+	+			+	+					
Selaginella	+			+	+	+	+			+	+					
Lycopodium	+	+		+	+	+				+	+					+
Huperzia	+	+		+	+					+						+
Anthoceros	+			+	+	+										
Phaeoceros	+			+	+	+										
Megaceros	+			+	+	+										
Physcomitrella			+	+	+							+	+	+	+	
Marchantia		+		+	+							+	+			

(Moniliformopses: Seed Plants, Ceratopteris, Platycerium, Psilotum; Lycopodiophyta: Equisetum, Selaginella, Lycopodium, Huperzia; Anthocerotophyta: Anthoceros, Phaeoceros, Megaceros; Bryophyta: Physcomitrella; Marchantiophyta: Marchantia)

Fig. 7. Diversity of branching patterns and subunit compositions of xyloglucans from the main lineages of land plants. A "+" indicates the presence of a structural element in the xyloglucan.

Glycosyl residue	Sidechain	R_1	R_2	R_3
β-D-Galp	L	-2)-α-D-Xylp-(1-	-H	-H
	F	-2)-α-D-Xylp-(1-	α-L-Fucp-(1-	-H
β-D-GalpA	P	β-D-Galp ↓ 4 -2)-α-D-Xylp-(1-	-H	-H
	Q	β-D-Galp ↓ 4 -2)-α-D-Xylp-(1-	-H	β-D-Galp-(1-
α-L-Arap	D	-2)-α-D-Xylp-(1-	-H	-H
	E	-2)-α-D-Xylp-(1-	α-L-Fucp-(1-	-H
	M	β-D-Galp ↓ 4 -2)-α-D-Xylp-(1-	-H	-H
	N	β-D-Galp-(1-6)-β-D-Galp ↓ 4 -2)-α-D-Xylp-(1-	-H	-H

Fig. 8. Structural homologies of β-D-galactopyranosyl, β-D-galactopyranosyl uronic acid, and α-L-arabinopyranosyl residues and oligosaccharide sidechain structures of land plant xyloglucans.

(Figure 8). Thus, horsetails and spike mosses likely have genes that encode proteins similar to the fucosyltransferase (FUT1, At2g03220) that adds a fucosyl residue to Gal in Arabidopsis XyG (Perrin et al. 1999, 2003). Indeed, the Selaginella genome contains several putative homologs (∼46% amino acid identity) of FUT1. The closest FUT1 homologs we detected in the Physcomitrella genome encode proteins with a somewhat lower amino acid identity (<33%), a result that is consistent with the lack of fucosyl residues in the XyG produced by this moss.

Previous studies have shown that grasses and some Lamiids normally produce XyGs that contain no discernible amounts of fucosyl residues (Hoffman et al. 2005). However, our data show that the ability to fucosylate XyG existed prior to the time when these plants diverged from other vascular plants. Thus, genes encoding the XyG-specific fucosyltransferases may have been eliminated from the genomes of some Lamiids and grasses. Alternatively, these plants may still contain the XyG-specific fucosyltransferases-encoding genes, but only express them in specific cells, at specific developmental stages, or under specific growth conditions. Indeed, there is evidence that suspension-cultured rice (Kato and Matsuda 1985) and tall fescue grass (*Festuca arundinacea* Schreber) cells (McDougall and Fry 1994) produce fucosylated XyGs. We have also detected small amounts of fucose in the XyG produced by suspension-cultured rice cells (Peña and York, unpublished results). Furthermore, the rice genome contains at least three genes with >52% identity to Arabidopsis FUT1 (http://rapdb.dna.affrc.go.jp/). Such results

suggest that fucosylation of XyG may be more common than previously believed, although functional characterization of the putative rice FUT1 genes is required to substantiate this claim.

Xyloglucan-specific glycosyltransferases in land plants

All XyGs characterized to date (York et al. 1996; Hantus et al. 1997; Ray et al. 2004; Hoffmann et al. 2005; Jia et al. 2005) have a cellulosic backbone composed of (1→4)-linked β-D-Glcp residues with a regular branching pattern in which at least two consecutive Glcp residues bear sidechains at O-6. A common evolutionary origin of this basic structure is supported by the occurrence in the bryophyte *P. patens* (http://genome.jgi-psf.org/Phypa1_1/Phypa1_1.home.html) and the lycopodiophyte *Selaginella moellendorffii* (http://genome.jgi-psf.org/Selmo1/Selmo1.home.html) of at least one gene that encodes a protein with ∼50% amino acid identity to CSLC4 (At3g28180), the glucan synthase that is believed to catalyze elongation of the XyG backbone in Arabidopsis (Cocuron et al. 2007). Physcomitrella and Selaginella also contain genes encoding proteins with ∼50% amino acid identity to the xyloglucan xylosyltransferases XXT1 (At3g62720) and XXT2 (At4g2500), which catalyze the transfer of Xyl from UDP-Xyl to the XyG backbone in Arabidopsis (Cavalier and Keegstra 2006). Together, these results are consistent with the notion that XyG appeared early in land plant evolution and that the presence of XyG in the cell wall conferred an as yet unidentified adaptive

advantage that allowed plants to colonize the terrestrial environment (Popper and Fry 2003).

Somewhat surprisingly, Arabidopsis plants carrying null mutations in the genes encoding xylosyltransferases, XXT1 and XXT2, have cell walls that contain little, if any, XyG yet grow and develop normally in the laboratory (Cavalier et al. 2008). However, the possibility cannot be discounted that the lack of a visible phentotype in *xxt1 xxt2* plants is a characteristic of Arabidopsis as no mutations that completely disrupt XyG biosynthesis in other plants have been characterized. Indeed, null mutations in orthologous human and mouse genes often lead to different phenotypes (Liao and Zhang 2008). The ability of the *xxt*1 *xxt*2 double mutant to survive without XyG is surprising, given that XyG is present in the walls of all avascular and vascular land plants and that many XyG structural motifs are conserved. Moreover, land plants have numerous genes encoding proteins including xyloglucan transglycosylase/hydrolases that are believed to have a role in XyG metabolism (Rose et al. 2002; Van Sandt et al. 2006, 2007; Fry, Mohler, et al. 2008). It is likely that XyG confers an as yet unidentified selective advantage to plants growing in the natural environment. Determining the ability of *xxt*1 *xxt*2 double mutant to grow and to compete with wild-type plants for several generations (Tautz 2000) under diverse environmental conditions may provide clues regarding the mechanisms by which conserved XyG structures contribute to the survival of land plants.

Many of the α-D-Xyl*p* residues in XyGs are themselves substituted at *O*-2 with either β-D-Gal*p* residue (**L** and **F** sidechains, Hoffman et al. 2005) or with α-L-Ara*p* (**D** and **E** sidechains, see Figure 6) which is a structural homolog of β-D-Gal*p* (see Figure 8). We have shown that a β-D-Gal*p*A residue, a second structural homolog of β-D-Gal*p*, is linked to O-2 of the α-D-Xyl*p* residue (**P** and **Q** sidechains, see Figure 3) in moss and liverwort XyGs. Thus, the addition to the xylosyl residue of glycoses with the β-D-galactopyrano or α-L-arabinopyrano configuration is a common feature of XyGs. The formation of the β-D-Gal*p*-(1→2)-α-D-Xyl*p* linkage in Arabidopsis XyG is catalyzed by two galactosyltransferases, MUR3 (At2g20370) and GT18 (At5g62220) (Madson et al. 2003; Li et al. 2004). The Physcomitrella and Selaginella genomes contain several putative *MUR3* and *GT18* homologs (45–56% amino acid sequence identity) that may encode the α-L-Ara*p* transferase, β-D-Gal*p*A transferase, and β-D-Gal*p* transferase involved in biosynthesis of the distinctive XyG sidechains of nonvascular and nonflowering vascular plants. However, the functional characterization of these genes will be required to substantiate this notion.

The **M**, **N**, **P**, and **Q** sidechains of Physcomitrella XyG contain the structurally homologous glycosyl residues β-D-Gal*p*, β-D-Gal*p*A, and α-L-Ara*p* (Figure 8). Based on known biosynthetic pathways, it is likely that these residues are added to XyG by glycosyltransferases that utilize UDP-α-D-Gal, UDP-α-D-GalA, and UDP-β-L-Ara*p* as donor substrates. Nevertheless, the possibility cannot be discounted that in mosses the β-D-Gal*p*A and α-L-Ara*p* are enzymically formed from β-D-Gal*p* after this residue has been added to the polymer. That is, C-6 oxidation of a β-D-Gal*p* residue would generate β-D-Gal*p*A. Decarboxylation of a β-D-Gal*p*A residue would form α-L-Ara*p* (see Figure 8). However, the absence of β-D-Gal*p*A residues together with the presence of α-L-Ara*p* residues in the XyGs produced *S. kraussiana* and *E. hyemale* (see Figure 4) suggests that in these vas-

cular plants the formation of α-L-Ara*p* does not occur by this mechanism.

Plants may optimize xyloglucan-cellulose interactions by controlling xyloglucan branching patterns, sidechain structures, and O-acetylation

Liverworts are believed to be the extant plants most closely related to the first plants to adapt to life on land (Qiu et al. 2006). Our studies indicate that the Marchantia synthesizes an XXGG-type XyG (50% branching) and that Physcomitrella produces an XXGGG-type XyG (40% branching). Thus, these branching patterns are likely to have evolved prior to the XXXG-type pattern (75% branching) that is characteristic of hornworts and many vascular plants.

The presence of sidechains makes XyG much more water soluble than cellulose and may facilitate the transport of the nascent XyG from the Golgi (Zhang and Staehelin 1992) to the cell wall (Moore et al. 1986), where it is then incorporated into the cellulose-XyG complex (Carpita and Gibeaut 1993). The XXGG- and XXGGG-type XyGs produced by liverworts and mosses, respectively, contain structurally complex sidechains with β-D-Gal*p*A and 2,4-linked α-D-Xyl*p* residues. The observation that anionic sidechains are more abundant in Physcomitrella XyG than in the more highly branched Marchantia XyG suggests that the anionic sidechains themselves attenuate XyG–XyG and/or XyG–cellulose interactions by a steric or coloumbic mechanism. Indeed, the ability of Tamarind XyG to hydrogen bond to cellulose is reduced when some of the nonxylosylated backbone glucosyl and sidechain galactosyl residues are chemically converted to glucosyluronic acid and galactosyluronic acid residues, respectively (Takeda et al. 2008). We suggest that the presence of uronic acid in XyG affect XyG–cellulose interactions and that other mechanisms to attenuate XyG–cellulose interactions appeared during the evolutionary events that led to the appearance of vascular plants.

We have shown that hornworts and many vascular plants produce highly branched XXXG-type XyGs with sidechains (**E** and **F**) that contain a terminal α-L-Fuc*p* residue. Thus, fucosylation of XyG is associated with a high degree of branching, consistent with the hypothesis (Levy et al. 1991; Hanus and Mazeau 2006) that fucosylation provides a mechanism to attenuate XyG binding to cellulose. The appearance of XXGGG- and XXGG-type XyGs in certain vascular plants, including the Poaceae and Lamiids (Kato et al. 1983; York et al. 1996; Hoffman et al. 2005), may be the result of independent reversions to the XyG branching patterns that are characteristic of mosses and liverworts. The XXGG- and XXGGG-type XyGs produced by Lamiids and Poaceae lack fucose. In fact, no fucose has been detected in XyGs with these branching patterns, nor is there evidence that XyGs produced by Lamiids, Poaceae, or any other vascular plant contain the acidic **P** and **Q** sidechains. Rather, many of the unbranched backbone β-D-Glc*p* residues are *O*-acetylated at O-6 in the XXGG- and XXGGG-type XyGs produced by vascular plants (York et al. 1996; Jia et al. 2005). The results of preliminary studies (unpublished results of the authors) indicate that Physcomitrella XyG is not *O*-acetylated. These observations suggest that *O*-acetyl substituents and α-D-Xyl*p* sidechains have comparable functions including attenuating the association of XyG molecules with each other or with cellulose. We propose that the biophysical properties of XyG

and the mechanics of its interaction with cellulose are determined in each plant species by optimizing the interactions of specific branching patterns, specific sidechain structures, and *O*-acetyl substituents. The nature of these biophysical properties is likely to be difficult to discern by examining isolated XyGs in solution, although they may have significant consequences within the topologically complex environment of the plant cell wall itself (O'Neill and York 2003; Hanus and Mazeau 2006).

In summary, we have shown that XyG is present in the walls of all land plants and that these XyGs have several common structural motifs. We have provided evidence that the XyGs of the Marchantiophyta and Bryophyta are unique in that they contain branched and acidic sidechains. Our structural characterization of XyGs from avascular and vascular plants is consistent with the notion that hornworts are sisters to the vascular plants. Additional studies of polysaccharides isolated from the walls of diverse plant lineages is likely to provide further insight into changes in wall structure that occurred during the evolution of land plants and how these polysaccharides contribute to plant growth and development.

Material and methods

Plant material

The plants used in this study were selected to represent the major divisions of avascular and seedless vascular plants. Tissue from actively growing protonema or leafy gametophore of the bryophytes and aerial portions of the sporophyte generation of lycopodiophytes and monilophytes were rinsed with water and stored at −80°C. *Marchantia polymorpha*, *Lycopodium tristachyum*, and *Huperzia lucidula* were obtained from the Carolina Biological Supply Co. (Carolina Biological Supply Company, Burlington NC). *Equisetum hyemale*, *Psilotum nudum*, *Platycerium bifurcatum*, and *Selaginella kraussiana* were obtained from the Plant Biology greenhouse, the University of Georgia. Specimens of *Phaeoceros sp.* and *Megaceros sp.* were provided by Yin-Long Qui (University of Massachusetts, MA).

Ceratopteris richardii spores were germinated in a liquid "C-Fern" medium (Carolina Biological Supply Company), and the gametophytes were grown for 12 days at 28°C under constant light. *Physcomitrella patens* (ecotype Gransden 2004) protonemata were grown with a 16 h light/8 h dark cycle at 22°C on cellophane-overlaid agar containing a modified BCD-ATG medium, containing 5 mM diammonium tartrate and 0.5% w/w glucose (Nishiyama et al. 2000). Leafy gametophytes were grown with a 16 h light/8 h dark cycle at 22°C on a solid-modified Knop's medium (Fu et al. 2007). *Anthoceros agrestis* was grown under constant light at 24 C in a modified Gamborg's B-5 medium containing 1% w/w sucrose (Petersen 2003).

Preparation of cell walls and isolation of xyloglucan

AIR was prepared and depectinated by treatment with endo-polygalacturonase and pectin methyl-esterase (Hoffman et al. 2005). The depectinated AIR was then treated for 24 h at room temperature with 1 N KOH and then with 4 N KOH containing 0.5% (w/v) NaBH$_4$. The alkali-soluble extracts were cooled, adjusted to pH 5 with glacial acetic acid, dialyzed (3500 MW cut-off tubing, Spectrum Laboratories, Rancho Dominguez, CA) against deionized water, and lyophilized. Most of the XyG was solubilized by 4 N KOH. Solutions of the 4 N KOH-soluble material, in 25 mM ammonium formate, pH 6.5, were eluted through a Q-sepharose anion-exchange column (1 × 10 cm) to remove pectic material (Hoffman et al. 2005). Somewhat unexpectedly the anionic XyG oligosaccharides were also eluted with 25 mM ammonium formate suggesting that they bind only weakly to the anion-exchange column.

Preparation and purification of Xyloglucan oligosaccharides (XyGOs)

The XyG-enriched fractions were treated with XEG (Novozymes, Bagsvaerd, Denmark) as described (Pauly et al. 1999) and the resulting XyGOs isolated using a Superdex-75 HR10/30 SEC column (GE Healthcare Bio-Sciences Corp. Piscataway, NJ) with refractive index detection (Knauer, Berlin, Germany). The column was eluted with 50 mM ammonium formate, pH 5, and the oligosaccharide-containing fractions were collected manually and lyophilized. Unless stated otherwise, the XyGOs were converted to their corresponding XyGols by treatment for 1 h at room temperature with NaBH$_4$ (250 μL of a 10 mg/mL solution in 1 M NH$_4$OH). The reaction was terminated by adding acetic acid and the XyGols then desalted using OnGuard H cartridges (Dionex Corp. Sunnyvale, CA).

P. patens XyGols were separated into acidic and neutral fractions using a Sephadex G-25 column (2.5 × 90 cm, GE Healthcare Bio-Sciences Corp. Piscataway, NJ) eluted with water. Fractions were collected manually and portions analyzed by MALDI-TOF-MS to locate the XyGols. Fractions containing neutral and acidic oligosaccharides were pooled separately and lyophilized.

E. hyemale XyGols and the neutral and acidic XyGols of *P. patens* were purified by reversed-phase HPLC on a Zorbax RP-18 column (25 × 10 cm, Agilent Technologies Inc. Santa Clara, CA) eluted with a gradient of aqueous MeOH (0–25% v/v over 25 min at 1 mL/min). The column was washed with aqueous 50% methanol for 10 min and then re-equilibrated in water. Oligosaccharides were detected using a Sedex 55 evaporative light scattering detector (Sedere, Alfortvile, France).

Structural characterization of xyloglucan oligosaccharides (XyGOs) and xyloglucan oligoglycosyl alditols (XyGols)

XyGOs or their corresponding XyGols were characterized by spectroscopic and chemical methods. The molecular weight of each purified XyGO or XyGol was determined by MALDI-TOF-MS. The 1D and 2D (gCOSY, TOCSY, and NOESY) spectra of each purified XyGol were recorded. The ^{1}H-^{13}C HSQC spectra were recorded if sufficient material was available. Isolated spin systems, corresponding to individual glycosyl residues, were identified and the chemical shifts and scalar coupling patterns were recorded (Tables I, II, and IV). These data were compared with data for well-characterized XyGols to identify sidechain structures and branching patterns that had previously been characterized. Unique structures were deduced by analysis of the isolated spin systems and their scalar and dipolar interactions with other spin systems. For example, glycosidic linkages were deduced by identifying long-range (interglycosidic) scalar coupling in the gCOSY spectra or interglycosidic dipolar coupling in the NOESY spectra. When mixtures of XyGols were analyzed, groups of resonances that arose from each component of the mixture were associated by signal integration,

as each pair of signals arising from a single chemical species should have a 1:1 intensity ratio. Whenever possible ^{1}H assignments were confirmed by assignment of one-bond heteronuclear scalar coupling observed in the HSQC spectra. Chemical shift effects (e.g., glycosylation shifts) typically provided information regarding the presence and location of glycosyl linkages, although spectral overlap occasionally prevented unambiguous assignment of glycosidic linkages.

Glycosyl-linkage composition analysis of XyGols
Galactosyluronic acid residues in *P. patens* XyGols were activated with *N-cyclohexyl-N'*-(2-morpholinoethyl)carbodiimide methyl-*p*-toluenesulfonate (Sigma-Aldrich, St Louis, MO) and then converted to 6,6-dideuteriogalactosyl residues by treatment with NaBD$_4$ (Carpita and McCann 1996). Carboxyl-reduced XyGols and other neutral XyGols were per-*O*-methylated using solid NaOH/CH$_3$I (Ciucanu and Costello 2003) with slight modifications. Suspensions of solid NaOH were prepared by vigorously mixing aqueous 50%NaOH (100 µL) and dry MeOH (200 µL) followed by the addition of dry dimethylsulfoxide (DMSO, 2 mL). The suspension was centrifuged, and the pellet was washed with DMSO (5 × 2 mL) and finally suspended in dry DMSO (2 mL).

The per-*O*-methylated XyGols were isolated from the reaction mixture by extraction with chloroform. Per-*O*-methylated XyGols were converted to their methylated alditol acetates (Carpita and Shea 1989). Glycosyl-residue and glycosyl-linkage compositions were determined by gas chromatography electron-impact mass spectrometry (York et al. 1985).

Determination of the absolute configuration of the glycosyl residues
The absolute configurations of the glycosyl residues in the XyGols were determined by ^{1}H-NMR spectroscopic analysis of the chiral per-*O*-(*S*)-2-methylbutyrate derivatives (York et al. 1997).

Nuclear magnetic resonance spectroscopy
The NMR spectra of XyGOs and XyGol mixtures and purified XyGols in D$_2$O (0.6 mL, 99.9%; Cambridge Isotope Laboratories, Andover, MA) in 5 mm NMR tubes were recorded using a Varian Inova-NMR spectrometer (Varian Inc, Palo Alto, CA) operating at 600 MHz at a sample temperature of 298 K. The 2D spectra were recorded using standard Varian pulse programs. Chemical shifts were measured relative to internal acetone (δ 2.225). Intraglycosidic scalar couplings and long-range (interglycosidic) scalar couplings were simultaneously detected in the gCOSY spectra of the XyGols recorded at high resolution (Jia et al. 2005). Interglycosidic dipolar couplings for XyGols were observed in the NOESY spectra recorded using a mixing time of 200 ms. Data were processed using MastRe-C software (Universidad de Santiago de Compostela, Spain).

MALDI-TOF and ESI mass spectrometry
XyGOs and XyGols were analyzed by MALDI-TOF-MS (Peña et al. 2007) using an Applied Biosystems Voyager-DE Biospectrometer (Applied Biosystems, Foster City, CA). Solutions of per-*O*-methylated XyGols in aqueous 50% methanol containing 1 mM NaOH were analyzed by ESI-MS in the positive ion mode using a Thermo-Fisher LTQ mass spectrometer (ThermoScien-

tific, Waltham, MA). Samples were infused into the source at 0.4 µL/min and electrosprayed through a 30 µm SilicaTip™ emitter (New Objective, Woburn MA) operated at 2.0 kV. ESI-MS-MS was performed using normalized collision energy of 28%, activation Q of 0.25, and activation time of 30 ms.

Supplementary Data

Supplementary data for this article is available online at http://glycob.oxfordjournals.org/.

Conflict of interest statement

None declared.

Abbreviations

AIR, alcohol insoluble residue; Ara*f*, arabinofuranosyl; Ara*p*, arabinopyranosyl; DMSO, dimethylsulfoxide, ESI-MS, electrospray ionization mass spectrometry; Fuc*p*, fucopyranosyl; FUT1, fucosyltransferase 1; Gal*p*, galactopyranosyl; Gal*p*A, galatopyranosyluronic acid; Glc*p*, glucopyranosyl; HPLC, high-performance liquid chromatography; MALDI-TOF-MS, matrix-assisted laser-desorption time-of-flight mass spectrometry; NMR, nuclear magnetic resonance; XXT1, xyloglucan xylosyltransferase 1; XXT2, xyloglucan xylosyltransferase 2; XyG, xyloglucan; XyGO, xyloglucan oligosaccharide; XyGol, xyloglucan oligosaccharide-alditol; Xyl*p*, xylopyranosyl.

References

Bouche N, Bouchez D. 2001. *Arabidopsis* gene knockout: Phenotypes wanted. *Curr Opin Plant Biol.* 4:111–117.
Carfa A, Duckett JG, Knox JP, Ligrone R. 2005. Distribution of cell-wall xylans in bryophytes and tracheophytes: New insights into basal interrelationships of land plants. *New Phytol.* 168:231–240.

Carpita NC, Gibeaut DM. 1993. Structural models of primary cell walls in flowering plants: Consistency of molecular structure with the physical properties of the walls during growth. *Plant J*. 3:1–30.

Carpita NC, McCann MC. 1996. Some new methods to study plant polyuronic acids and their esters. In: Townsend R, Hotchkiss A, editors. *Progress in Glycobiology*. New York: Dekker. p. 595–611.

Carpita NC, Shea EM. 1989. Linkage structure of carbohydrates by gas chromatography-mass spectrometry (GC-MS) of partially methylated alditol acetates. In: Biermann CJ, McGinnis GD, editors. *Analysis of Carbohydrates by GLC and MS*. Baton Rouge, FL: CRC Press. p. 157–215.

Cavalier DM, Keegstra K. 2006. Two xyloglucan xylosyltransferases catalyze the addition of multiple xylosyl residues to cellohexaose. *J Biol Chem*. 281:34197–34207.

Cavalier DM, Lerouxel O, Neumetzler L, Yamauchi K, Reinecke A, Freshour G, Zabotina OA, Hahn MG, Burgert I, Pauly M et al. 2008. Disrupting two *Arabidopsis thaliana* xylosyltransferase genes results in plants deficient in xyloglucan, a major primary cell wall component. *Plant Cell*. 20:1519–1537.

Ciucanu I, Costello CE. 2003. Elimination of oxidative degradation during the per-*O*-methylation of carbohydrates. *J Am Chem Soc*. 125:16213–16219.

Cocuron J-C, Lerouxel O, Drakakaki G, Alonso AP, Liepman AH, Keegstra K, Raikhel N, Wilkerson CG. 2007. A gene from the cellulose synthase-like C family encodes a β-1,4 glucan synthase. *Proc Natl Acad Sci USA*. 104:8550–8555.

Duff R J, Villareal JC, Cargill DC, Renzaglia KS. 2007. Progress and challenges toward developing a phylogeny and classification of the hornworts. *Bryologist*. 110:214–243.

Fry SC, Mohler KE, Nesselrode BHWA, Franková L. 2008. Mixed-linkage β-glucan: Xyloglucan endotransglucosylase, a novel wall-remodelling enzyme from Equisetum (horsetails) and charophytic algae. *Plant J*. 55:240–252.

Fry SC, Nesselrode BHWA, Miller JG, Mewburn BR. 2008. Mixed-linkage (1→3,1→4)-β-D-glucan is a major hemicellulose of Equisetum (horsetail) cell walls. *New Phytol*. 179:104–115.

Fry SC, York WS, Albersheim P, Darvill AG, Hayasi T, Joseleau J-P, Kato Y, Lorences EP, Maclachlan GA, McNeil M et al. 1993. An unambiguous nomenclature for xyloglucan-derived oligosaccharides. *Physiol Plant*. 89:1–3.

Fu H, Yadav MP, Nothnagel EA. 2007. *Physcomitrella patens* arabinogalactan proteins contain abundant terminal 3-*O*-methyl-L-rhammosyl residues not found in angiosperms. *Planta*. 226:1511–1524.

Gibeaut DM, Pauly M, Bacic T, Fincher GB. 2004. Changes in cell wall polysaccharides in developing barley (*Hordeum vulgare*) coleoptiles. *Planta*. 221:729–738.

Glushka JN, Terrell M, York WS, O'Neill MA, Gucwa A, Darvill AG, Albersheim P, Prestegard JH. 2003. Primary structure of the 2-*O*-methyl-α-fucose-containing side chain of the pectic polysaccharide, rhamnogalacturonan II. *Carbohydr Res*. 338:341–352.

Hantus S, Pauly M, Darvill AG, Albersheim P, York WS. 1997. Structural characterization of novel L-galactose-containing oligosaccharide subunits of jojoba seed xyloglucans. *Carbohydr Res*. 304:11–20.

Hanus J, Mazeau K. 2006. The xyloglucan-cellulose assembly at the atomic scale. *Biopolymers*. 82:59–73.

Hoffman M, Jia Z, Peña MJ, Cash M, Harper A, Blackburn AR, Darvill AG, York WS. 2005. Structural analysis of xyloglucan in the primary cell walls of plants in the subclass *Asteridae*. *Carbohydr Res*. 340:1826–1840.

Huether CM, Lienhart O, Baur A, Stemmer C, Gorr G, Reski R, Decker EL. 2005. Glyco-engineering of moss lacking plant-specific sugar residues. *Plant Biol*. 7:292–299.

Jia Z, Cash M, Darvill AG, York WS. 2005. NMR characterization of endogenously *O*-acetylated oligosaccharides isolated from tomato (*Lycopersicon esculentum*) xyloglucan. *Carbohydr Res*. 340:1818–1825.

Jia Z, Qin Q, Darvill AG, York WS. 2003. Structure of the xyloglucan produced by suspension-cultured tomato cells. *Carbohydr Res*. 328:1197–1208.

Kato Y, Ito S, Iki K, Matsuda K. 1983. Xyloglucan and β-D-glucan in cell walls of rice seedlings. *Plant Cell Physiol*. 23:351–364.

Kato Y, Matsuda K. 1985. Xyloglucan in the cell walls of suspension-cultured rice cells. *Plant Cell Physiol*. 26:437–445.

Lee KJD, Sakata Y, Mau S-L, Pettolino F, Bacic A, Quatrano RS, Knight CD, Knox JP. 2005. Arabinogalactan proteins are required for apical cell extension in the moss *Physcomitrella patens*. *Plant Cell*. 17:3051–3065.

Levy S, York WS, Stuike-Prill R, Meyer B, Staehelin LA. 1991. Simulations of the static and dynamic molecular conformations of xyloglucan. The role of the fucosylated sidechain in surface-specific sidechain folding. *Plant J*. 1:195–215.

Li X, Cordero I, Caplan J, Mølhøj M, Reiter W-D. 2004. Molecular analysis of 10 coding regions from Arabidopsis that are homologous to the MUR3 xyloglucan galactosyltransferase. *Plant Physiol*. 134:940–950.

Liao B-Y, Zhang J. 2008. Null mutations in human and mouse orthologs frequently result in different phenotypes. *Proc Natl Acad Sci USA*. 105:6987–6992.

Ligrone R, Vaughn KC, Renzaglia KS, Knox JP, Duckett JG. 2002. Diversity in the distribution of polysaccharide and glycoprotein epitopes in the cell walls of bryophytes: New evidence for the multiple evolution of water-conducting cells. *New Phytol*. 156:491–508.

Madson M, Dunand C, Li X, Verma R, Vanzin GF, Caplan J, Shoue DA, Carpita NC, Reiter W-D. 2003. The MUR3 gene of Arabidopsis encodes a xyloglucan galactosyltransferase that is evolutionarily related to animal exostosins. *Plant Cell*. 15:1662–1670.

Matsunaga T, Ishii T, Matsumoto H, Darvill AG, Albersheim P, O'Neil MA. 2004. Occurrence of the primary cell wall polysaccharide rhamnogalacturonan II in pteridophytes, lycopodiophytes, and bryophytes. Implications for evolution of vascular plants. *Plant Physiol*. 134:1–13.

McDougall GJ, Fry SC. 1994. Fucosylated xyloglucan in suspension-cultured cells of the graminaceous monocotyledon, *Festuca arundinacea*. *J Plant Physiol*. 143:591–595.

Moore PJ, Darvill AG, Albersheim P, Staehelin LA. 1986. Immunogold localization of xyloglucan and rhamnogalacturonan I in the cell walls of suspension-cultured sycamore cells. *Plant Physiol*. 82:787–794.

Niklas KJ. 2004. The cell walls that bind the tree of life. *BioScience*. 54:831–841.

Nishiyama T, Hiwatashi Y, Sakakibara K, Kato M, Hasebe M. 2000. Tagged mutagenesis and gene-trap in the moss *Physcomitrella patens* by shuttle mutagenesis. *DNA Res*. 7:9–17.

O'Neill MA, York WS. 2003. The composition and structure of plants primary cell walls. In: Rose JKC, editor. *The Plant Cell Wall*. Oxford: Blackwell. p. 1–54.

Pauly M, Albersheim P, Darvill A, York WS. 1999. Molecular domains of the cellulose/xyloglucan network in the cell walls of higher plants. *Plant J*. 20:629–639.

Peña MJ, Zhong R, Zhou G-K, Richardson EA, O'Neill MA, Darvill AG, York WS, Ye Z-H. 2007. *Arabidopsis irregular xylem8* and *irregular xylem9*: Implications for the complexity of glucuronoxylan biosynthesis. *Plant Cell*. 19:549–563.

Perrin RM, DeRocher AE, Bar-Peled M, Zheng W, Norambuena L, Orellana A, Raikhel NV, Keegstra K. 1999. Xyloglucan fucosyltransferase, and enzyme involved in plant cell wall biosynthesis. *Science*. 284:1976–1979.

Perrin RM, Jia Z, Wagner TA, O'Neill MA, Sarria R, York WS, Raikhel NV, Keegstra K. 2003. Analysis of xyloglucan fucosylation in Arabidopsis. *Plant Physiol*. 132:768–778.

Petersen M. 2003. Cinanamic acid 4-hydroxylase from cell cultures of the hornwort *Anthoceros agrestis*. *Planta*. 217:96–101.

Popper ZA. 2008. Evolution and diversity of green plant cell walls. *Curr Opin Plant Biol*. 11:286–292.

Popper ZA, Fry SC. 2003. Primary cell wall composition of bryophytes and charophytes. *Ann Bot*. 91:1–12.

Popper ZA, Fry SC. 2004. Primary cell wall composition of pteridophytes and spermatophytes. *New Phytol*. 164:165–174.

Popper ZA, Fry SC. 2005. Widespread occurrence of a covalent linkage between xyloglucan and acidic polysaccharides in suspension-cultured angiosperm cells. *Ann Bot*. 96:91–99.

Popper ZA, Sadler IH, Fry SC. 2001. 3-*O*-Methyl-D-galactose residues in lycopodiophyte primary cell walls. *Phytochemistry*. 57:711–719.

Qiu Y-L, Li L, Wang B, Chen Z, Knoop V, Groth-Malonek M, Dombrovska O, Lee J, Kent L, Rest J et al. 2006. The deepest divergences in land plants inferred from phylogenomic evidence. *Proc Natl Acad Sci USA*. 103:15511–15516.

Quatrano RS, McDaniel SF, Khandelwal A, Perroud P-F, Cove DJ. 2007. *Physcomitrella patens*: Mosses enter the genomic age. *Curr Opin Plant Biol*. 10:182–189.

Ray B, Loutelier-Bourhis C, Lange C, Condamine E, Driouich A, Lerouge P. 2004. Structural investigation of hemicellulosic polysaccharides from *Argania spinosa*: Characterisation of a novel xyloglucan motif. *Carbohydr Res*. 339:201–208.

Rose JKC, Braam J, Fry SC, Nishitani K. 2002. The XTH family of enzymes involved in xyloglucan endotransglucosylation and endohydrolysis: Current perspectives and a new unifying nomenclature. *Plant Cell Physiol*. 43:1421–1435.

Schaefer DG, Zrÿd J-P. 2001. The moss *Physcomitrella patens*, now and then. *Plant Physiol*. 127:1430–1438.

Sørensen I, Pettolino FA, Wilson SM, Doblin MS, Johansen B, Bacic A, Willats WGT. 2008. Mixed-linkage (1→3),(1→4)-β-D-glucan is not unique to the Poales and is an abundant component of *Equisetum arvense* cell walls. *Plant J*. 54:510–521.

Takeda T, Miller JG, Fry SC. 2008. Anionic derivatives of xyloglucan function as acceptor but not donor substrates for xyloglucan endotransglucosylase activity. *Planta*. 227:893–905.

Tautz D. 2000. A genetic uncertainty problem. *Trends Genet*. 16:475–477.

Thompson JE, Fry SC. 2000. Evidence for covalent linkage between xyloglucan and acidic pectins in suspension-cultured rose cells. *Planta*. 211:275–286.

Van Sandt VST, Guisez Y, Verbelen J-P, Vissenberg K. 2006. Analysis of a xyloglucan endotransglycosylase/hydrolase (XTH) from the lycopodiophyte *Selaginella kraussiana* suggests that XTH sequence characteristics and function are highly conserved during the evolution of vascular plants. *J Exp Bot*. 57:2909–2922.

Van Sandt VST, Stieperaere H, Guisez Y, Verbelen J-P, Vissenberg K. 2007. XET activity is found near sites of growth and cell elongation in Bryophytes and some green algae: New insights into the evolution of primary cell wall elongation. *Ann Bot*. 99:39–51.

Vanzin GF, Madson M, Carpita NC, Raikhel NV, Keegstra K, Reiter W-D. 2002. The *mur2* mutant of *Arabidopsis thaliana* lacks fucosylated xyloglucan because of a lesion in fucosyltransferase AtFUT1. *Proc Natl Acad Sci USA*. 99:3340–3345.

York WS, Darvill AG, McNeil M, Stsevenson TT, Albersheim P. 1985. Isolation and characterization of plant cell walls and cell wall components. *Meth Enzymol*. 118:3–40

York WS, Hantus S, Albersheim P, Darvill AG. 1997. Determination of the absolute configuration of monosaccharides by ^{1}H NMR spectroscopy of their per-*O*-(*S*)-2-methylbutyrate derivatives. *Carbohydr Res*. 300:199–206.

York WS, Kolli VSK, Orlando R, Albersheim P, Darvill AG. 1996. The structure of arabinoxyloglucans produced by solanaceous plants. *Carbohydr Res*. 285:99–128.

York WS, van Halbeek H, Darvill AG, Albersheim P. 1990. Sturctural analysis of xyloglucan oligosaccharides by [1]H-n.m.r. spectroscopy and fast-atom-bombardment mass spectrometry. *Carbohydr Res*. 200:9–31.

Zablackis E, York WS, Pauly M, Hantus S, Reiter W-D, Chapple CCS, Albersheim P, Darvill A. 1996. Substitution of L-fucose by L-galactose in cell walls of *Arabidopsis mur1*. *Science*. 272:1808–1810.

Zhang GF, Staehelin LA. 1992. Functional compartmentation of the Golgi apparatus of plant cells. Immunocytochemical analysis of high-pressure frozen- and freeze-substituted Sycamore Maple suspension culture cells. *Plant Physiol*. 99:1070–1083.